Biochemical and Biophysical Research Communications 429 (2012) 24–30

Contents lists available at SciVerse ScienceDirect

Biochemical and Biophysical Research Communications

journal homepage: www.elsevier.com/locate/ybbrc

Nuclear PIM1 confers resistance to rapamycin-impaired endothelial proliferation

Thomas Walpen [a], Ina Kalus [a], Jürg Schwaller [b], Martin A. Peier [a], Edouard J. Battegay [a,c], Rok Humar [a,c,*]

[a] Research Unit, Division Internal Medicine, University Hospital Zürich, 8091 Zürich, Switzerland
[b] Department of Biomedicine, University of Basel, 4031 Basel, Switzerland
[c] Zurich Center for Integrative Human Physiology (ZIHP), 8057 Zürich, Switzerland

ARTICLE INFO

Article history:
Received 18 October 2012
Available online 3 November 2012

Keywords:
Endothelial cells
Rapamycin
mTOR
PIM1
Nucleus
Proliferation

ABSTRACT

The PIM serine/threonine kinases and the mTOR/AKT pathway integrate growth factor signaling and promote cell proliferation and survival. They both share phosphorylation targets and have overlapping functions, which can partially substitute for each other. In cancer cells PIM kinases have been reported to produce resistance to mTOR inhibition by rapamycin. Tumor growth depends highly on blood vessel infiltration into the malignant tissue and therefore on endothelial cell proliferation. We therefore investigated how the PIM1 kinase modulates growth inhibitory effects of rapamycin in mouse aortic endothelial cells (MAEC).

We found that proliferation of MAEC lacking *Pim1* was significantly more sensitive to rapamycin inhibition, compared to wildtype cells. Inhibition of mTOR and AKT in normal MAEC resulted in significantly elevated PIM1 protein levels in the cytosol and in the nucleus. We observed that truncation of the C-terminal part of *Pim1* beyond Ser 276 resulted in almost exclusive nuclear localization of the protein. Re-expression of this *Pim1* deletion mutant significantly increased the proliferation of $Pim1^{-/-}$ cells when compared to expression of the wildtype *Pim1* cDNA. Finally, overexpression of the nuclear localization mutant and the wildtype *Pim1* resulted in complete resistance to growth inhibition by rapamycin.

Thus, mTOR inhibition-induced nuclear accumulation of PIM1 or expression of a nuclear C-terminal PIM1 truncation mutant is sufficient to increase endothelial cell proliferation, suggesting that nuclear localization of PIM1 is important for resistance of MAEC to rapamycin-mediated inhibition of proliferation.

1. Introduction

The kinase complexes built by mammalian target of rapamycin (mTOR), mTOR complex 1 (mTORC1) and mTOR complex 2 (mTORC2), are central to the control of cell growth, proliferation and metabolism. mTOR signaling is intertwined with AKT/PKB signaling, since AKT induces mTORC1 activity and mTORC2 directly phosphorylates AKT [1]. Many studies on rapamycin, a potent inhibitor of mTOR complex 1 (mTORC1) for cancer therapy, revealed that inhibitory effects of rapamycin and derivatives on tumor growth remain restricted to specific cancer subtypes and have not a generally extended efficacy [2]. Resistance to rapamycin and derivates may be caused by redundant signaling pathways. In the past, several mechanisms have been identified, which possibly counteract rapamycin-induced growth arrest including mutations in mTOR regulating activities but also angiogenesis-associated mechanisms [3,4]. Therefore, these molecular targets could serve for combined drug therapy to improve the efficacy of anti-cancer treatments.

Like mTOR and AKT, PIM kinases also belong to the class of serine/threonine kinases [5]. The family of PIM kinases consists of three members, PIM1, PIM2 and PIM3, which have overlapping functions [6–9]. They are constitutively active and have been found to be overexpressed in different tumors, promoting cell proliferation and survival [10]. Both, the mTOR/AKT and PIM signaling pathways share phosphorylation targets such as B-cell-lymphoma-2-antagonist of cell death (BAD) or proline-rich Akt substrate of 40 kDa (PRAS40) [11–17]. Interestingly, PIM kinases can substitute for mTOR-mediated signaling. Rapamycin had a minimal effect on T-cell expansion in vitro and in vivo, but cells from $Pim1^{-/-}/Pim2^{-/-}$ animals displayed an unexpected sensitivity to rapamycin [18]. In animal lymphoma models AKT-mediated chemoresistance was abrogated with rapamycin, whereas chemoresistance caused by PIM was refractory to rapamycin treatment [19]. Additionally, it has been shown that *Pim1* depletion decreased the potential of AKT-mediated survival signaling: in the myocardium of mice PIM1 expression increases after acute pathological injury and was also elevated in failing hearts of both mice and humans, suggesting a reparative function of the PIM1 kinase in

* Corresponding author at: Division of Internal Medicine, Gloriastrasse 30/GLO30-J14, CH-8091 Zürich, Switzerland. Fax: +41 (0) 44 634 53 39.
E-mail address: Rok.Humar@usz.ch (R. Humar).

0006-291X/$ - see front matter © 2012 Elsevier Inc. All rights reserved.
http://dx.doi.org/10.1016/j.bbrc.2012.10.106

the myocardium. Indeed, overexpression of *Pim1* in the myocardium protected mice from infarction injury and myocardial apoptosis. Cardioprotective stimuli associated with AKT activation induced PIM1 expression, but could not protect the myocardium in *Pim1*$^{-/-}$ mice [20].

Endothelial cells are particularly important for reparative processes being the starting point of angiogenesis, the growth of new microvessels. The neovasculature provides nutrients, oxygen and removes waste products to ensure reparation of the injured tissue. Likewise growing tumors equally acquires neovasculature upon transformation into a malignant phenotype. Therefore, the functions of PIM1 in endothelial cells need to be explored. In endothelial cells PIM1 is transiently expressed during in vivo angiogenesis and induced by vascular endothelial growth factor (VEGF) in human umbilical vein endothelial cells (HUVECs). Furthermore, *Pim1* silencing impaired vascular endothelial growth factor-A (VEGF-A)-induced proliferation and migration and inhibited capillary formation on matrigel and endothelial cell sprouting in HUVECs [21]. We have demonstrated recently, that PIM1 performs an important function in endothelial cell adhesion [22]. Here we have investigated whether PIM1 affects mTOR inhibition-mediated growth arrest in mouse aortic endothelial cells (MAEC).

2. Materials and methods

2.1. Cell culture and transfection

MAEC were isolated from aortae of FVB/N wildtype and *Pim1*$^{-/-}$ mouse strains as described previously [23]. For all experiments cell culture dishes were coated with 0.1% gelatine gold (Carl Roth GmbH, Karlsruhe, Germany) for 20 min at 37 °C. Cells were maintained in DMEM (Biochrom, Berlin, Germany) complemented with 10% FBS, 1% sodium pyruvate, 1% non-essential amino acids and 1% penicillin–streptomycin (Invitrogen, LuBioScience GmbH, Luzern, Switzerland). Cell numbers were assessed with a NucleoCounter® NC-100™ (Chemometec, Allerød, Denmark). In all experiments the cells were washed with phosphate-buffered saline (Invitrogen) after 24 h of seeding and trypsinized (TripLE express, Invitrogen) for further processing. Light micrographic pictures were acquired using an IX71 inverted microscope (Olympus, Volketswil, Switzerland). For PIM1 overexpression cDNA encoding the particular human PIM1 variants was subcloned into a *pCMV-Tag2A* expression vector (Stratagene) and cell transfection was performed with 500 ng of vector/reaction using a basic endothelial cells nucleofector kit in a Nucleofector II device (Amaxa Biosystems, Cologne, Germany) according to the manufacturers protocol.

2.2. Immunoblotting

Total cell lysates were prepared using RIPA buffer as described before [23]. After SDS–PAGE, proteins were transferred onto polyvinylidene fluoride (PVDF) membrane (Millipore, Billerica, MA). The membrane was blocked with 4% skim milk powder in TBS-Tween solution or 4% BSA and probed with following antibodies: rabbit polyclonal anti-PIM1 (Cell Signaling Technology, Danvers, MA), rabbit polyclonal anti-α-Tubulin (Cell Signaling Technology, Danvers, MA), rabbit polyclonal anti-Histone H3 (Cell Signaling Technology, Danvers, MA), and mouse monoclonal anti-β-actin (Sigma–Aldrich, St. Louis, MO). Anti-mouse or rabbit-HRP-conjugated IgGs (Cell Signaling Technology, Danvers, MA) were used for visualization of relevant proteins on X-ray films by a chemiluminescence reaction (Thermo Scientific, Waltham, MA).

2.3. Fluorescence imaging

The cells were fixed in 4% paraformaldehyde for 20 min at 37 °C on coverslips (Karl Hecht AG, Sondheim, Germany) and then permeabilized with 0.5% Triton X-100 in PBS for 10 min. After blocking for 45 min with goat serum the cells were incubated with the following antibodies: mouse monoclonal to PIM1 12H8 (Santa Cruz, Santa Cruz, CA), mouse monoclonal to FLAG (Sigma–Aldrich, St. Louis, MO) and the nuclei were stained with Hoechst 33342 (Invitrogen). After three washing steps cells were incubated with Alexa Fluor 555-conjugated secondary antibody (Invitrogen). The coverslips were then mounted with FluorSave™ (Merck, Darmstadt, Germany) on glass slides (Thermo Scientific, Waltham, MA). Fluorescence imaging was performed using a ZEISS fluorescence microscope (Carl Zeiss AG, Oberkochen, Germany) and a confocal laser scanning microscope Leica SP5 (Leica, Wetzlar, Germany).

2.4. Cloning

Full length *Pim1* was subcloned from *pCMV-Tag 2A* into *pdsRED-Pim1*. *Pim1* truncation mutants were generated by PCR cloning (primer sequences are available upon request) using the PfuTurbo® DNA-polymerase (Stratagene, La Jolla, CA). All mutants were fully sequence-verified.

2.5. Proliferation assay

4×10^3 MAEC/well were plated in 96-well cell culture dishes (TPP, Trasadingen, Switzerland) o/n. Cells were washed three times with PBS and 24 h starved in DMEM without FCS. Then rapamycin or diluent was added for 1 h and subsequently FCS was added to the cells cultures in a final dilution of 10%. Proliferation was measured with the metabolic indicator WST-1 (Roche, Basel, Switzerland), which was added at 24 h after rapamycin treatment according to the manufacturers protocol. The degree of proliferation was determined using SpectraMax microplate reader (Molecular Devices, Sunnyvale, CA), measuring the absorbance at 450 nm. Control wells contained DMEM with appropriate rapamycin concentrations to provide a background level measurement.

2.6. Kinase inhibitors and extraction of cytosolic and nuclear fractions

To inhibit protein kinases of different signaling pathways, the cells were seeded and grown overnight, as described in cell culture methods. Afterwards the cells were washed three times with PBS and 24 h starved in DMEM without FCS. Then the appropriate inhibitor or diluent was added for 1 h and subsequently FCS was added to the cells cultures in a final dilution of 10%. (Concentrations of the inhibitors: Akt inhibitor IV 1 μM, $G\ddot{o}_{6983}$ 1 μM, U_{0126} 5 μM, $GSK3_{IX}$ 1 μM, Rapamycin 0.25 μM, LY_{294002} 5 μM). After 3 h the cells were harvested and cytosolic and nuclear fractionation was performed with a NE-PER nuclear and cytoplasmic extraction kit (Thermo Scientific, Waltham, MA), according to the manufacturers protocol.

2.7. FACS analysis

The apoptosis assay was performed using a Fluoresceinisothiocyanat (FITC) Annexin V/Dead cell apoptosis kit (Invitrogen, Carlsbad, Ca). Therefore the cells were harvested and washed in cold PBS. After centrifugation the cells were resuspended in 1X Annexin-binding buffer to a density of $\sim 1 \times 10^6$ cells/mL. According to the protocol 5 μl of FITC Annexin V and 1 μl of the 100 μg/mL Propidium iodide (PI) working solution were added to each 100 μl of cell suspension. After 15 min incubation at room temperature, 400 μl of 1X Annexin-binding buffer was added to each sample and the tubes were kept on ice until sorting. The samples were then analyzed with a FACSCalibur (Becton Dickinson, Franklin Lakes, NJ) at emission wave-lengths of 530 nm and >575 nm.

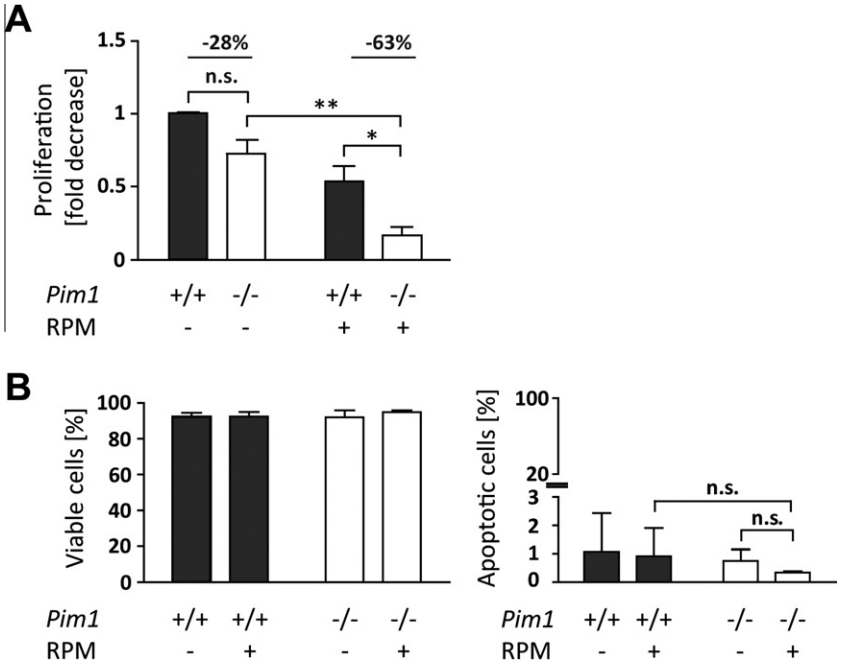

Fig. 1. Cell proliferation and apoptosis of wildtype vs. *Pim1*$^{-/-}$ endothelial cells. (A) Fold decrease cell proliferation of wildtype compared to *Pim1*$^{-/-}$ MAEC treated with 250 nM rapamycin (RPM) and control. (B) FACS analysis of corresponding treatment conditions of wildtype vs. *Pim1*$^{-/-}$ cells. Wildtype cells (black bars), *Pim1*$^{-/-}$ cells (white bars). Data are represented as means ± s.e.m. ($n = 3$). $^{*}P < 0.05$, $^{**}P < 0.01$.

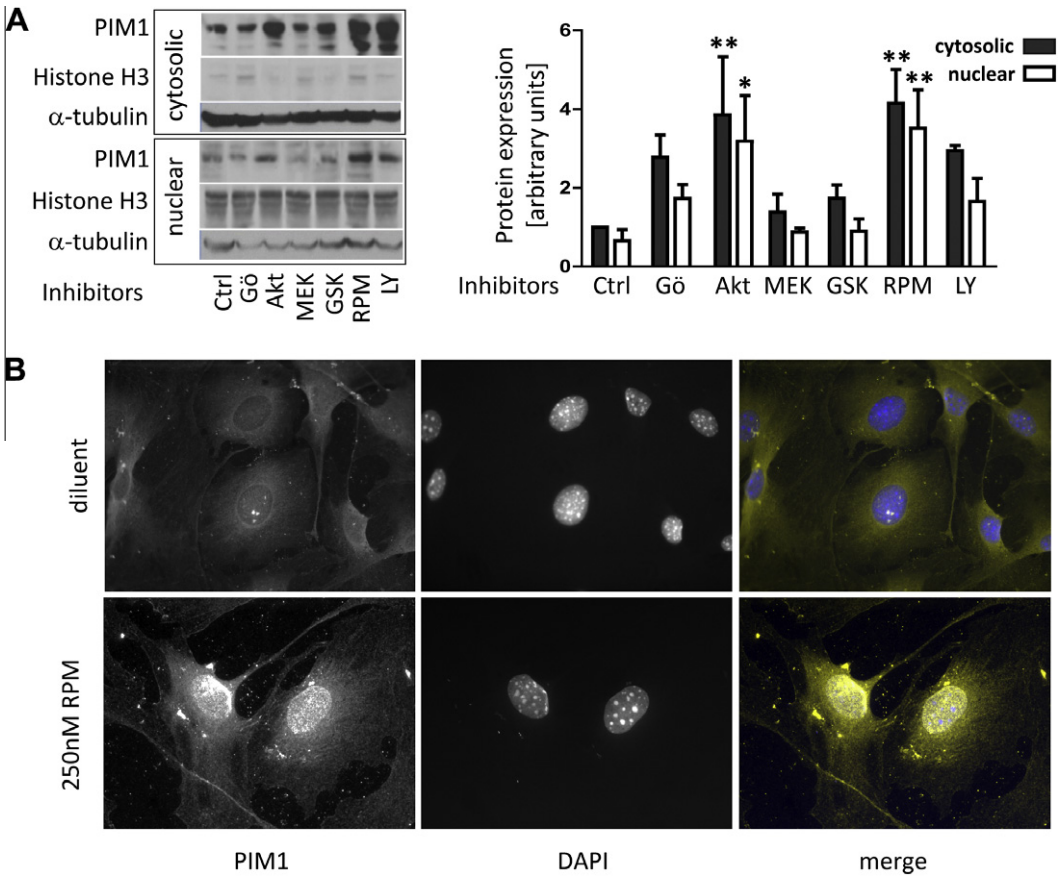

Fig. 2. AKT and mTOR inhibition increases PIM1 expression levels. (A) PIM1 expression levels of cytosolic and nuclear fractions from MAEC treated with inhibitors of different signaling cascades (left panel). Corresponding densitometric quantification of PIM1 expression levels. (right panel) (B) Immunofluorescence image of endogenous PIM1 after 3 h of rapamycin treatment (lower panel) and control (upper panel). Endogenous PIM1 (left panel), nuclei (middle panel) and merge (right panel). In the merge picture the nuclei are displayed in blue and PIM1 kinase in yellow. Data are represented as means ± s.e.m. ($n = 3$). $^{*}P < 0.05$, $^{**}P < 0.01$.

2.8. Statistical analysis and software

All statistical tests were performed using GraphPad Prism 5.04 for Windows (GraphPad software, San Diego, CA). The Western blots were quantified using Image J software. For analysis of repeated measurements a two way Anova followed by a Bonferroni post test was performed. Differences between two groups were evaluated using unpaired *t*-test. To compare more than two groups one way anova followed by a Bonferroni post test was done. Data are represented as means ± sem.

3. Results

3.1. Pim1 deletion enhances the inhibitory effect of rapamycin on endothelial cell proliferation

Wildtype and *Pim1*$^{-/-}$ MAEC were treated for 24 h with rapamycin (RPM) and cellular proliferation, viability and apoptosis was quantified (Fig. 1). Proliferation of *Pim1*$^{-/-}$ cells decreased by 28 ± 0.1% compared to wildtype cells (Fig. 1A). Upon treatment with rapamycin the proliferation of the cells decreased by 63 ± 0.1% in comparison to wildtype cells (Fig. 1A). Thus, we found a 1.3-fold and a 3.2-fold decrease in proliferation after rapamycin treatment in wildtype and PIM1 knockout MAECs, respectively. To exclude a possible toxic effect of rapamycin resulting in reduced cell numbers due to apoptosis, we also analyzed cell viability (Fig. 1B). We observed no significant changes in viability of wildtype or *Pim1*$^{-/-}$ cells after rapamycin treatment (Fig. 1B left panel). Under all conditions more than 90% cells remained viable. Accordingly, no significant increase of the apoptotic cell population was observed, upon treatment of wildtype and *Pim1*$^{-/-}$ cells with rapamycin (Fig. 1B right panel). In all conditions tested the percentage of apoptotic cells was less than 1.2%.

3.2. mTOR and AKT inhibition increases PIM1 protein expression

To investigate whether inhibition of proliferation directly affects PIM1 protein levels in MAEC, we treated wildtype cells with several established small molecule kinase inhibitors involved in different signaling cascades known to affect cellular growth (Fig. 2A). We measured cytosolic and nuclear PIM1 localization (Fig. 2) and we quantified PIM1 protein expression levels of the cytosolic and nuclear fractions after 3 h of treatment with the inhibitors. We found that inhibition of mTOR by rapamycin or AKT by Akt inhibitor IV significantly increased PIM1 protein levels both in cytosolic and nuclear fractions with no significant changes of subcellular distribution (Fig. 2A). Compared to controls PIM1 was upregulated 3.9-fold after AKT inhibition and 4.2-fold after mTOR inhibition by rapamycin in the cytosolic fractions and 4.7-fold and 5.2-fold, in nuclear fractions, respectively. Although not reaching statistical significant, we also observed upregulation of PIM1 upon inhibition of Phosphatidylinositide 3-kinase (PI3 K) by LY_{294002} and Protein kinase C by $Gö_{6983}$. Similar to the results by immunoblotting we also observed upregulation of PIM1 in the cytoplasm and the nucleus after 3 h of rapamycin treatment by immunofluorescence staining (Fig. 2B).

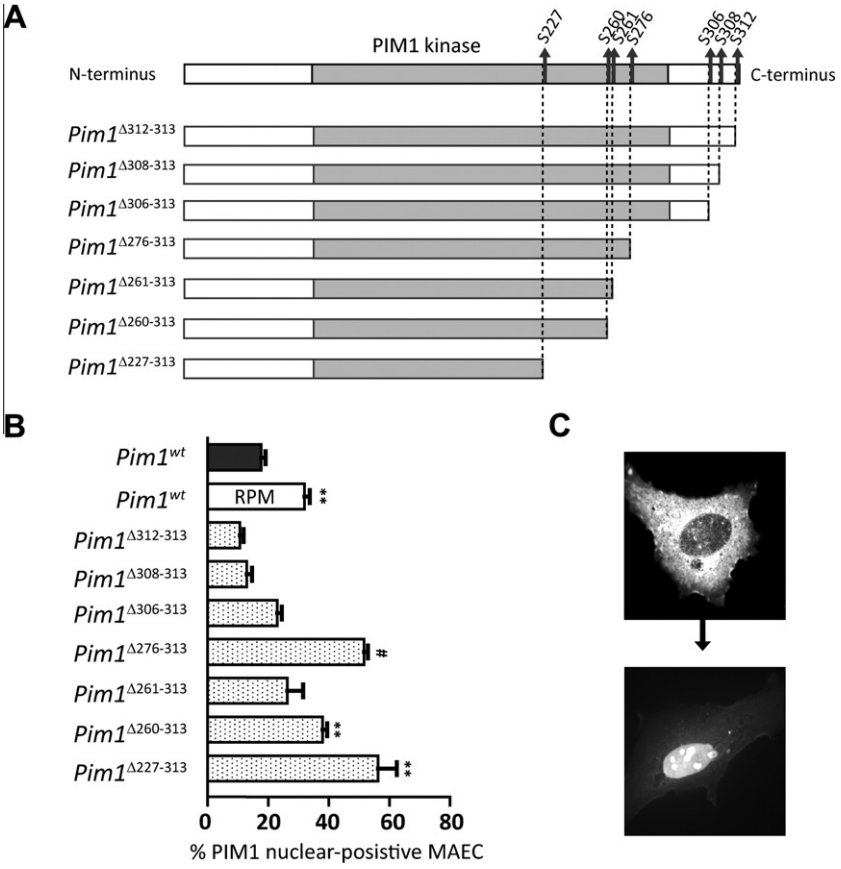

Fig. 3. C-terminal truncation sites of PIM1 kinase and percentage of nuclear PIM1 positive *Pim1*$^{-/-}$ cell cultures, transfected with dsRED-*Pim1* cDNA. (A) Schematical representation of PIM1 kinase and the C-terminal truncation mutants. (B) Percentage of *Pim1* nuclear-positive *Pim1*$^{-/-}$ MAEC transfected with dsRED-*Pim1* wildtype (black bar), dsRED-Pim1 wildtype with RPM (open bar) and C-terminal truncation mutants *Pim1*$^{\Delta 313-227}$ (spotted bar). (C) dsRED-*Pim1* transfected *Pim1*$^{-/-}$ MAEC, untreated (upper panel) and treated with rapamycin (lower panel). Data are represented as means ± s.e.m. ($n = 3$). Data are represented as means ± s.e.m. ($n = 3$). $^{*}P < 0.05$, $^{**}P < 0.01$, $^{\#}P < 0.0001$.

Taken together, MAEC lacking PIM1 are more sensitive to inhibition of proliferation by rapamycin; and blocking mTOR by rapamycin or AKT by Akt inhibitor IV significantly increases cytosolic and nuclear PIM1 protein levels in wildtype cells.

3.3. C-terminal truncation of Pim1 beyond Serine 276 (*Pim1*$^{\Delta 276-313}$) increases nuclear localization of PIM1

PIM1 nuclear localization has been proposed to depend on the integrity of its carboxy terminus (C-terminus) [24]. To identify critical sites, i.e., minimal critical C-terminal domains responsible for PIM1 nuclear localization, we generated several *Pim1* carboxy-terminal PIM1 deletion mutants (schematically shown in Fig. 3A).

Full-length dsRED-*Pim1* (*Pim1*^{wt}) or dsRED-*Pim1* truncation mutants (*Pim1*$^{\Delta 227-313}$) were expressed in *Pim1*$^{-/-}$ MAEC. Cells positive for nuclear PIM1 protein were quantified by immunofluorescence microscopy (Fig. 3B). Cell cultures of MAEC expressing *Pim1*^{wt}, treated for 3 h with rapamycin, displayed a 1.88-fold increase in nuclear PIM1, compared to untreated cells. MAEC transfected with *Pim1*$^{\Delta 312-313}$, *Pim1*$^{\Delta 308-313}$ and *Pim1*$^{\Delta 306-313}$ showed no significant increase in nuclear PIM1 positive cells. However, except for MAEC transfected with truncation mutant *Pim1*$^{\Delta 260-313}$, C-terminal truncations beyond Serine 276, displayed a significantly higher percentage of PIM1 nuclear positive cells: *Pim1*$^{\Delta 276-313}$ 2.9-fold, *Pim1*$^{\Delta 260-313}$ 2.2-fold and *Pim1*$^{\Delta 227-313}$ 3.2-fold compared to *Pim1*^{wt} transfected cells. Fig. 3C shows representative immunofluorescent pictures of cells either negative (upper panel) or positive (lower panel) for dsRED-*Pim1*.

3.4. Truncation of C-terminal residues of FLAG-Pim1 beyond Serine 276 (*Pim1*$^{\Delta 276-313}$) results in nuclear localization of the kinase and increases MAEC proliferation independent of rapamycin.

To exclude effects of the N-terminally fused monomeric red fluorescent protein we performed the experiment with FLAG-tagged *Pim1* constructs that were expressed in *Pim1*$^{-/-}$ cells (Fig. 4A). Fluorescence microscopy using anti-FLAG antibodies confirmed that only *Pim1* truncations beyond serine 276 resulted in significant nuclear translocation (Fig. 4A lower panel), whereas smaller truncations inclusively *Pim1*^{wt} retained an even

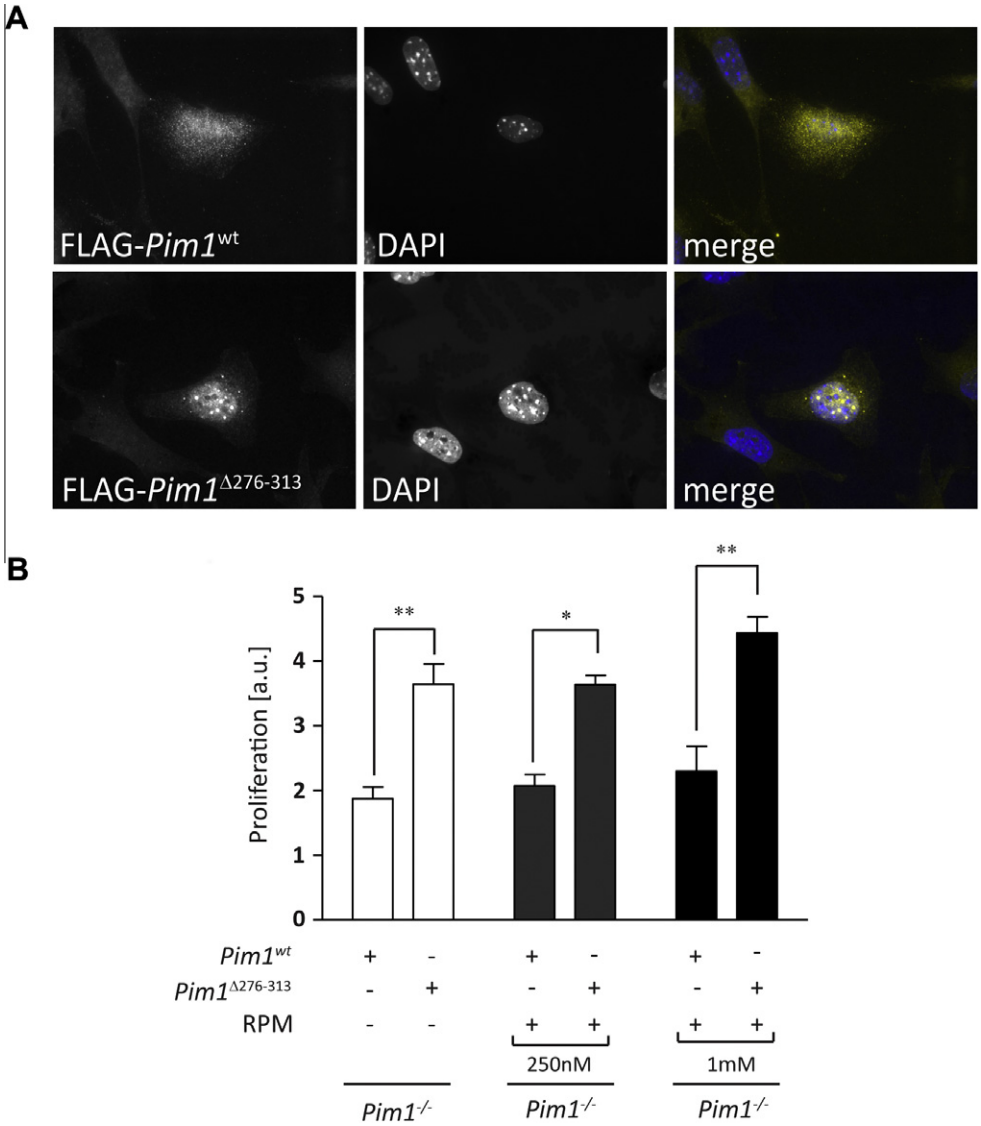

Fig. 4. FLAG-*Pim1*$^{\Delta 276-313}$ localizes to the nucleus. (A) MAEC transfected with FLAG-*Pim1*^{wt} (upper panel) and FLAG-*Pim1*$^{\Delta 276-313}$ (lower panel) cDNA. FLAG-*Pim1* (left panel), nuclei (middle panel) and merge (right panel). In the merge picture the nuclei are displayed in blue and PIM1 kinase in yellow. (B) Proliferation measurement of *Pim1*$^{-/-}$ MAEC re-expressing FLAG-*Pim1*^{wt} and FLAG-*Pim1*$^{\Delta 276-313}$, untreated and treated with 250 nM and 1 mM rapamycin. Data are represented as means ± s.e.m. ($n = 3$). Data are represented as means ± s.e.m. ($n = 3$). $^{*}P < 0.05$, $^{**}P < 0.01$.

distribution of PIM1 between the cytosol and the nucleus (Fig. 4A upper panel). We therefore chose the FLAG-*Pim1*$^{\Delta 276-313}$ truncation mutant that was consistently found in the nucleus to perform proliferation experiments. FLAG-*Pim1*^{wt} and FLAG-*Pim1*$^{\Delta 276-313}$ were overexpressed in *Pim1*$^{-/-}$ cells and cell proliferation was assessed (Fig. 4C left panel). Interestingly, *Pim1*$^{-/-}$ MAEC expressing FLAG-*Pim1*$^{\Delta 276-313}$ displayed a 1.94-fold higher proliferation than cells expressing full length FLAG-*Pim1*. *Pim1*$^{-/-}$ MAEC expressing FLAG-*Pim1*^{wt} or *Pim1*$^{\Delta 276-313}$were additionally treated with 250 nM and 1 mM rapamycin, respectively (Fig. 4B middle and left panel). Interestingly the increase in proliferation of *Pim1*$^{-/-}$ MAEC expressing *Pim1*$^{\Delta 276-313}$ was not diminished by rapamycin treatment.

4. Discussion

Rapamycin and several analogs are being evaluated as anticancer agents in clinical trials. Results indicate that many human cancers have intrinsic resistance and tumors initially sensitive to rapamycin become refractory. Inhibition of mTOR has direct effects on the growth of cancer cells but also influences tumor angiogenesis, i.e. endothelial proliferation and motility [25]. Here we examined the potential role of PIM1 kinase in conferring resistance to mTOR inhibition in endothelial cells.

PIM kinases are ubiquitously expressed and increased expression has been demonstrated to contribute to tumor progression of non- and hematological origin, by promoting proliferation, survival and drug resistance [26]. Tumor progression highly depends on blood vessel infiltration and thereby on endothelial cell proliferation [27]. PIM1 kinase has been shown to contribute to VEGF induced proliferation in HUVECs [21]. Furthermore, PIM1 can substitute for the inhibitory effect of rapamycin in malignant lymphoma [19]. Therefore, we asked, whether there could be such a refractory mechanism to rapamycin-mediated mTOR inhibition in endothelial cells. Indeed, compared to wildtype cells, *Pim1*$^{-/-}$ MAEC proliferation showed a significantly increased sensitivity to rapamycin (Fig. 1A). PIM kinases also mediate survival signaling by interaction with members of the BCL2 protein family [28] and partially through direct phosphorylation of the pro-apoptotic protein BAD [12,20]. However, the effect of rapamycin on MAEC cell proliferation is independent of cell death, as we observed no significant differences in cell viability (Fig. 1B).

Intriguingly, inhibition of the mTOR signaling pathway by rapamycin or mTOR-associated AKT significantly increased PIM1 levels in the cytosol and the nuclear compartment. PIM1 kinase has been found to be cytosolic, nuclear or both [29,30]. However, the significance of different subcellular localizations of PIM1 are not yet fully elucidated. In cardiac explants from murine neonates and mice in the early adulthood PIM1 seems to shift from a predominantly nuclear to a more cytoplasmic localization, whereas in adults PIM1 expression is almost lost. However in a mouse model of chronic heart failure the percentage of nuclear PIM1 again markedly increased, which was also the case in samples from failing human hearts [20]. In lymphoma cells PIM1 appeared to be predominantly nuclear, which was not the case in normal lymph nodes [24]. Furthermore, irradiation promoted nuclear translocation of PIM1 in radioresistant squamocellular cancers of head and neck [31]. Taken together, nuclear cellular localization of PIM1 kinase may correlate with proliferating cancer cells and survival response upon pathologic injury. Therefore we were interested to dissect, whether nuclear PIM1 contributes for the significantly different proliferative response to rapamycin of *Pim1*$^{+/+}$ and *Pim1*$^{-/-}$ cells. Ionov et al. [24] proposed that half of the carboxy-terminus of PIM1 kinase being responsible for PIM1 nuclear translocation. Therefore we generated a series of C-terminal *Pim1* deletion mutants to identify critical sites for PIM1 nuclear translocation. We found significant differences in the nuclear abundance of dsRED-*Pim1*^{wt} and the different dsRED-*Pim1* truncation mutants, even though the number of nuclear positive cells did not excess 56%. Baird et al. showed that dsRED oligomerizes in live cells, with a tendency to aggregate at least to tetramers [32]. This could constrain cellular trafficking of the protein fused to dsRED, thus the diffusion or the transport of dsRED-PIM1 through the nuclear pore complex. To diminish such side effects, we repeated the experiment with FLAG-epitope tagged PIM variants. Indeed MAEC transfected with FLAG-*Pim1*, displayed an almost complete nuclear localization of PIM1 truncated beyond Ser 276, as compared to cells expressing dsRED-*Pim1*. Taken together we show, that a site N-terminal to serine 276 is critical for PIM1 cellular localization. Intriguingly, expression of the nuclear PIM1 mutant resulted in an almost twofold increase in proliferation over wildtype PIM1 overexpression, which was insensitive to rapamycin. Since overexpression of the wildtype *Pim1* also results in partial nuclear translocation we argue, that rapamycin insensitivity is primarily dependent on nuclear *Pim1* localization.

In conclusion, our findings could potentially explain one of the mechanisms leading to rapamycin-resistance: Rapamycin and mTOR-signaling related inhibition increases the expression of PIM1 resulting in higher nuclear PIM1 protein levels. Importance of the nuclear localization of PIM1 is demonstrated by a C-terminal deletion mutant that localizes to the nucleus, and counteracts the anti-proliferative effect of rapamycin.

Acknowledgments

This work was supported by a grant from the Swiss National Science Foundation to Edouard J. Battegay and from the University of Zürich (contract grant number: 31003A-118349). We thank A. Berns and M.C. Nawijn who kindly provided the FVB/N wildtype and *Pim1*$^{-/-}$ mouse strains (The Netherlands Cancer Institute, Amsterdam, Netherlands).

References

[1] M. Laplante, D.M. Sabatini, mTOR signaling in growth control and disease, Cell 149 (2012) 274–293.
[2] D. Benjamin, M. Colombi, C. Moroni, et al., Rapamycin passes the torch: a new generation of mTOR inhibitors, Nat. Rev. Drug Discovery 10 (2011) 868–880.
[3] R.T. Kurmasheva, S. Huang, P.J. Houghton, Predicted mechanisms of resistance to mTOR inhibitors, Br. J. Cancer 95 (2006) 955–960.
[4] S.Y. Sun, L.M. Rosenberg, X. Wang, et al., Activation of Akt and eIF4E survival pathways by rapamycin-mediated mammalian target of rapamycin inhibition, Cancer Res. 65 (2005) 7052–7058.
[5] M. Bachmann, T. Moroy, The serine/threonine kinase Pim-1, Int. J. Biochem. Cell Biol. 37 (2005) 726–730.
[6] M.L. Breuer, H.T. Cuypers, A. Berns, Evidence for the involvement of Pim-2, a new common proviral insertion site, in progression of lymphomas, EMBO J. 8 (1989) 743–748.
[7] J.D. Feldman, L. Vician, M. Crispino, et al., KID-1, a protein kinase induced by depolarization in brain, J. Biol. Chem. 273 (1998) 16535–16543.
[8] H. Mikkers, J. Allen, P. Knipscheer, et al., High-throughput retroviral tagging to identify components of specific signaling pathways in cancer, Nat. Genet. 32 (2002) 153–159.
[9] N.M. van der Lugt, J. Domen, E. Verhoeven, et al., Proviral tagging in E mu-myc transgenic mice lacking the Pim-1 proto-oncogene leads to compensatory activation of Pim-2, EMBO J. 14 (1995) 2536–2544.
[10] M.C. Nawijn, A. Alendar, A. Berns, For better or for worse: the role of Pim oncogenes in tumorigenesis, Nat. Rev. Cancer 11 (2011) 23–34.
[11] C.J. Fox, P.S. Hammerman, C.B. Thompson, Fuel feeds function: energy metabolism and the T-cell response, Nat. Rev. Immunol. 5 (2005) 844–852.
[12] T.L. Aho, J. Sandholm, K.J. Peltola, et al., Pim-1 kinase promotes inactivation of the pro-apoptotic Bad protein by phosphorylating it on the Ser112 gatekeeper site, FEBS Lett. 571 (2004) 43–49.
[13] S.R. Datta, H. Dudek, X. Tao, et al., Akt phosphorylation of BAD couples survival signals to the cell-intrinsic death machinery, Cell 91 (1997) 231–241.
[14] L. del Peso, M. Gonzalez-Garcia, C. Page, et al., Interleukin-3-induced phosphorylation of BAD through the protein kinase Akt, Science 278 (1997) 687–689.

[15] A. Macdonald, D.G. Campbell, R. Toth, et al., Pim kinases phosphorylate multiple sites on Bad and promote 14–3-3 binding and dissociation from Bcl-XL, BMC Cell Biol. 7 (2006) 1.
[16] E.B. Nascimento, M. Snel, B. Guigas, et al., Phosphorylation of PRAS40 on Thr246 by PKB/AKT facilitates efficient phosphorylation of Ser183 by mTORC1, Cell. Signalling 22 (2010) 961–967.
[17] F. Zhang, Z.M. Beharry, T.E. Harris, et al., PIM1 protein kinase regulates PRAS40 phosphorylation and mTOR activity in FDCP1 cells, Cancer Biol. Ther. 8 (2009) 846–853.
[18] C.J. Fox, P.S. Hammerman, C.B. Thompson, The Pim kinases control rapamycin-resistant T cell survival and activation, J. Exp. Med. 201 (2005) 259–266.
[19] J.H. Schatz, E. Oricchio, A.L. Wolfe, et al., Targeting cap-dependent translation blocks converging survival signals by AKT and PIM kinases in lymphoma, J. Exp. Med. 208 (2011) 1799–1807.
[20] J.A. Muraski, M. Rota, Y. Misao, et al., Pim-1 regulates cardiomyocyte survival downstream of Akt, Nat. Med. 13 (2007) 1467–1475.
[21] A. Zippo, A. De Robertis, M. Bardelli, et al., Identification of Flk-1 target genes in vasculogenesis: Pim-1 is required for endothelial and mural cell differentiation in vitro, Blood 103 (2004) 4536–4544.
[22] T. Walpen, M. Peier, E. Haas, et al., Loss of Pim1 imposes a hyperadhesive phenotype on endothelial cells, Cell Physiol. Biochem. 30 (2012) 1083–1096.
[23] R. Humar, F.N. Kiefer, H. Berns, et al., Hypoxia enhances vascular cell proliferation and angiogenesis in vitro via rapamycin (mTOR)-dependent signaling, FASEB J. 16 (2002) 771–780.
[24] Y. Ionov, X. Le, B.J. Tunquist, et al., Pim-1 protein kinase is nuclear in Burkitt's lymphoma: nuclear localization is necessary for its biologic effects, Anticancer Res. 23 (2003) 167–178.
[25] M. Guba, P. von Breitenbuch, M. Steinbauer, et al., Rapamycin inhibits primary and metastatic tumor growth by antiangiogenesis: involvement of vascular endothelial growth factor, Nat. Med. 8 (2002) 128–135.
[26] Y. Alvarado, F.J. Giles, R.T. Swords, The PIM kinases in hematological cancers, Expert Rev. Hematol. 5 (2012) 81–96.
[27] P. Carmeliet, R.K. Jain, Angiogenesis in cancer and other diseases, Nature 407 (2000) 249–257.
[28] J.H. Song, A.S. Kraft, Pim kinase inhibitors sensitize prostate cancer cells to apoptosis triggered by Bcl-2 family inhibitor ABT-737, Cancer Res. 72 (2012) 294–303.
[29] L. Brault, T. Menter, E.C. Obermann, et al., PIM kinases are progression markers and emerging therapeutic targets in diffuse large B-cell lymphoma, Br J Cancer 107 (2012) 491–500.
[30] Y. Xie, K. Xu, B. Dai, et al., The 44 kDa Pim-1 kinase directly interacts with tyrosine kinase Etk/BMX and protects human prostate cancer cells from apoptosis induced by chemotherapeutic drugs, Oncogene 25 (2006) 70–78.
[31] K. Peltola, M. Hollmen, S.M. Maula, et al., Pim-1 kinase expression predicts radiation response in squamocellular carcinoma of head and neck and is under the control of epidermal growth factor receptor, Neoplasia 11 (2009) 629–636.
[32] G.S. Baird, D.A. Zacharias, R.Y. Tsien, Biochemistry, mutagenesis, and oligomerization of DsRed, a red fluorescent protein from coral, Proc. Natl. Acad. Sci. USA 97 (2000) 11984–11989.